DTU Library

Magneto-elastic coupling in La(Fe, Mn, Si)13Hy within the Bean-Rodbell model

Neves Bez, Henrique; Nielsen, Kaspar Kirstein; Norby, Poul; Smith, Anders; Bahl, Christian R. H.

[Link back to DTU Orbit](https://orbit.dtu.dk)

Magneto-elastic coupling in La(Fe, Mn, Si)13Hy within the Bean-Rodbell model

Henrique N. Bez, Kaspar K. Nielsen, Poul Norby, Anders Smith, and Christian R. H. Bahl

Articles you may be interested in

Sensitivity study of multi-layer active magnetic regenerators using first order magnetocaloric material La(Fe,Mn,Si)13Hy
J. Appl. Phys. 118, 014903 (2015); 10.1063/1.4923356

Dynamics of the magneto structural phase transition in La(Fe0.9Co0.015Si0.085)13 observed by magneto-optical imaging
J. Appl. Phys. 115, 17A925 (2014); 10.1063/1.4866880

Age splitting of the La(Fe1−xSix)13Hy first order magnetocaloric transition and its thermal restoration
J. Appl. Phys. 113, 17A908 (2013); 10.1063/1.4794976

Influence of particle size on the hydrogenation in La(Fe, Si)13 compounds
J. Appl. Phys. 113, 17A911 (2013); 10.1063/1.4794975

Occurrence of magneto-elastic coupling across the metal-insulator transition in LaMnO3±δ
AIP Conf. Proc. 1447, 1113 (2012); 10.1063/1.4710397

Magneto-elastic coupling in La(Fe, Mn, Si)$_{13}$H$_y$ within the Bean-Rodbell model

Henrique N. Bez,[a] Kaspar K. Nielsen, Poul Norby, Anders Smith, and Christian R. H. Bahl
Department of Energy Conversion and Storage, Technical University of Denmark - Frederiksborgvej 399, DK-4000 Roskilde - Denmark

First order magnetic phase transition materials present a large magnetocaloric effect around the transition temperature, where these materials usually undergo a large volume or structural change. This may lead to some challenges for applications, as the material may break apart during field change, due to high internal stresses. A promising magnetocaloric material is La(Fe, Mn, Si)$_{13}$H$_y$, where the transition temperature can be controlled through the Mn amount. In this work we use XRD measurements to evaluate the temperature dependence of the unit cell volume with a varying Mn amount. The system is modelled using the Bean-Rodbell model, which is based on the assumption that the spin-lattice coupling depends linearly on the unit cell volume. This coupling is defined by the model parameter η, where for $\eta > 1$ the material undergoes a first order transition and for $\eta \leq 1$ a second order transition. We superimpose a Gaussian distribution of the transition temperature with a standard deviation $\sigma(T_0)$, in order to model the chemical inhomogeneity. Good agreement is obtained between measurements and model with values of $\eta \sim 1.8$ and $\sigma(T_0) = 1.0$ K. © *2016 Author(s). All article content, except where otherwise noted, is licensed under a Creative Commons Attribution 3.0 Unported License.* [http://dx.doi.org/10.1063/1.4944400]

I. INTRODUCTION

The magnetocaloric effect (MCE) is a thermal response of a material when subjected to an applied magnetic field change.[1] Some materials may undergo a first order phase transition (FOPT) while others a second order (SOPT).[2] One of the FOPT materials series is the La-Fe-Si based alloys.[3] This alloy presents excellent MCE,[4] high thermal conductivity[5] and low thermal hysteresis[4] when compared to other FOPT magnetocaloric materials. Still, even with promising magnetocaloric performance, this family of materials presents some issues which have yet to be fully understood. During the phase transition the material has a volume change[6] that may break the sample apart.[7,8] Moreover, this material may present virgin behavior,[8] which is related to the microstructure of the material and the volume change.

The magnetoelastic modelling of such materials is of interest in order to predict and understand the behavior of them when cycled thermally and magnetically. Literature has shown[9] that the Bean-Rodbell model[10] can be applied for isotropic crystal structures such as NaZn$_{13}$. In this model the exchange constant, and therefore the Curie temperature, T_C, is in fact varied linearly with the lattice spacing as $T_C = T_0 \left[1 + \beta \frac{V - V_0}{V_0} \right]$, where V is the unit cell volume, and T_0 is the Curie temperature of the system when V is constrained to V_0, which is the volume at 0 K in the absence of strains introduced internally, e.g. by exchange interactions, or externally e.g. applied stresses. β is a parameter that controls the spin-lattice coupling strength. From the model, another important parameter that may be extracted is η. This parameter determines the order of the transition and is given by:

[a]hnbe@dtu.dk

6, 056217-1

$$\eta = 40\rho_s \kappa T_0 k_B \beta^2 \frac{(J(J+1))^2}{(2J+1)^4 - 1}. \tag{1}$$

Here ρ_s is the density of spins in the volume V, κ is the compressibility, k_B is the Boltzmann constant and J is the total angular momentum. η relates to the order of transition so that when $\eta \leq 1$ the material undergoes a SOPT and $\eta > 1$ a FOPT. Moreover the model predicts the following relationship between volume and magnetization $\frac{V - V_0}{V_0} = \rho_s \kappa k_B T_0 \beta \sigma^2 / 2 - P\kappa$, where σ is the normalized magnetization in respect to the saturation and P is the external applied pressure.

We here evaluate the volume change that the FOPT $La(Fe, Mn, Si)_{13}H_y$ presents by means of X-ray diffraction (XRD) at different temperatures. We also evaluate the nature of the phase transition by isofield magnetization measurements of single particles and multiple particles of the material, observing the effect that collective versus singular properties has. Finally, we use the Bean-Rodbell model to investigate the magnetoelastic coupling of these materials.

II. EXPERIMENTAL PROCEDURE

Three different compositions of $LaFe_{13-x-y}Mn_xSi_yH_{1.65}$ alloys were provided by Vacuumschmelze GmbH, with $x = 0.25, 0.22$ and 0.06; $y = 1.28, 1.23$ and 1.18, respectively. The materials as received are in the form of irregular shaped particles with a mean diameter of 560 ± 200 μm. From calorimetric measurements, not shown here, T_C was found to be 304.1, 314.1 and 340.3 K in the three samples, respectively. The different materials were analysed in a Rigaku Smartlab XRD as a function of temperature during heating and cooling procedures, under Cu radiation and in powder form. The measurements were done every 1 K, at stable temperature and without overshooting. Using the WINPOW software, Rietveld refinement[13] was performed to calculate the lattice parameters and phase fractions in each temperature for each material.

A LakeShore VSM, model 7407, was used to measure isofield magnetizations around the transition temperature (possible ~0.15 K overshooting). Low temperature magnetization was measured in a high field VSM (Cryogen Free Measurement System - 16 T) at 10 K from 0 to 10 T, with a rate of 1.7 mT/s. This measurement was used to calculate the total angular momentum, J. Isothermal entropy change, Δs, measurements were carried out in a custom-built DSC, using the temperature reset to account for hysteresis, described elsewhere.[12] Finally, the Bean-Rodbell model was applied with a normal distribution $\sigma(T_0)$ in order to take into account the chemical inhomogeneities.

III. RESULTS AND DISCUSSION

A. Experimental Results

XRD measurements were performed on three samples of $La(Fe, Mn, Si)_{13}H_y$, with slightly different concentrations of Mn, and therefore also Fe, Si and H. In order to properly refine the measured XRD, the ICSD-161853 was used for the $NaZn_{13}$-type crystal structure of $La(Fe, Mn, Si)_{13}H_y$ and for $\alpha - Fe$ we used ICSD-53802. The refinement was performed in the range $20° < 2\theta < 90°$, and all the present peaks were refined including the $\alpha - Fe$ ones. Due to the peak overlap around the phase transition, the PM phase was first refined at a temperature 2 K above the transition. Then, during the transition the obtained PM lattice parameter was fixed to that value. The refined patterns presented an average value of $R_p \sim 1.2$, $R_{wp} \sim 1.8$ and $\chi^2 \sim 9.2$. Figure 1 shows the XRD patterns for all the different measured temperatures during the cooling procedure for $x = 0.06$. The paramagnetic (PM) phase of this material family presents the same crystal structure as the ferromagnetic (FM) phase,[6] only the volume is changed by about 1% at the phase transition.[9] This means that the peaks measured in the XRD most probably overlap as observed in Fig. 1. Furthermore, the presence of both pairs of peaks (from FM and PM phase, respectively) means that there is a mixed state where some of the powder particles are in the FM state and others are still in the PM state.

From the refinements one can obtain the phase volumes and fractions. The materials had approximately 2 wt.% of $\alpha - Fe$ as a secondary phase. Figure 2 shows the unit cell volume as a function of the temperature for the three different materials. The first feature to notice is the volume
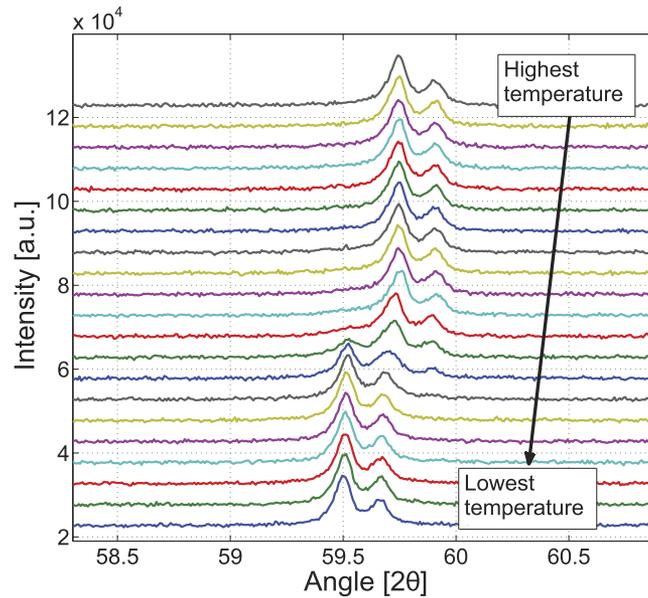
FIG. 1. XRD patterns for different fixed temperatures during the cooling procedure for $LaFe_{13-x-y}Mn_xSi_yH_{1.65}$ with $x = 0.06$. The reflection shown is for the peak (6 4 2).

change at T_C, explained in the introduction. One may also notice that for each sample there are temperatures where two unit cell volumes are plotted. These temperatures were the ones where FM and PM peaks overlapped as shown in Figure 1. Table I shows the volume change values for each material.

Figure 3 shows the FM fraction determined by Rietveld refinement as a function of the temperature for the three different materials studied. The error bars are mostly within the symbol size. The transitions seems to exhibit some thermal hysteresis, ΔT_{hyst}, but rather small. Furthermore, the transition occurs during a temperature span of about 6 K, rather than discontinuously.

To understand the transition of the material and any microstructural effects, magnetization measurements were carried out on three different particle distributions: (i) single particle, (ii) multiple single particles, and (iii) multiple ground particles (particle sizes of ∼25 μm). In case (i) and
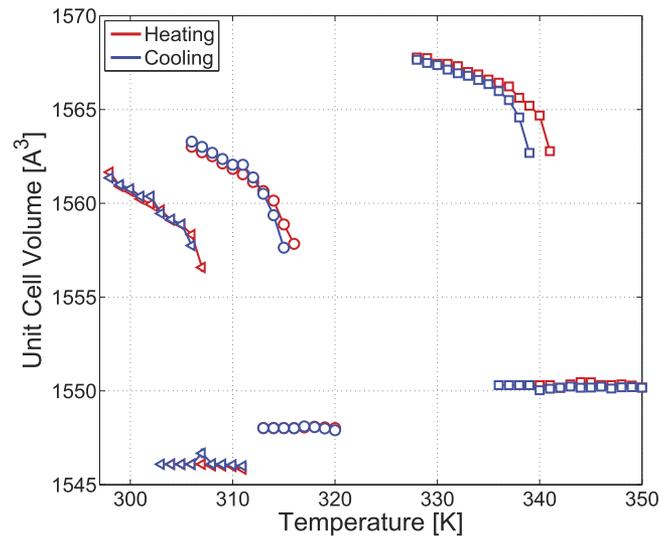

FIG. 2. Unit cell volume versus temperature for the three different materials during the cooling and heating procedures. The error bars are smaller than the symbol size.

TABLE I. Bean-Rodbell parameters and measured volume change. The parameters were found visually comparing modelled data and measured data.

x	0.25	0.22	0.06
T_0 [K]	290	300	320
$\sigma(T_0)$ [K]	1.0	1.0	0.8
η [-]	1.80	1.75	1.90
β [-]	35.93	34.81	34.83
V_0 [m^3]	$1.5460 \cdot 10^{-27}$	$1.5481 \cdot 10^{-27}$	$1.550 \cdot 10^{-27}$
ΔV [%]	0.82	0.83	1.04

(ii) the particles were glued to a rod inside an area of 4 by 4 mm, while in case (iii) the powder was put inside a cylindrical container. Figure 4 shows the magnetization measurements for $x = 0.06$, during the heating procedure. The different level of magnetization on the FM side is related to fluctuations of iron inside such small particles, and small differences in internal fields as the different particles have different demagnetization factors. Moreover, the virgin effect described elsewhere[8,11] was observed, and the samples were heated to above T_C prior to the measurements in order to avoid the virgin effect. As one may see, different single particles have different T_C, and when multiple raw particles (red dashed line) are measured the discrete behavior of the transition of single particles is observed as a plurality of sharp transitions within a few degrees. However, when the particles are ground to fine powder (blue line) with a mass of 101.3 mg, the properties change significantly, which is related to the microstructure as reported elsewhere.[14] When the powder is finely ground each single particle is, mostly, one single crystal. If one considers the presence of stoichiometry inhomogeneities, which virtually all materials possess, each single particle may have its own T_C, giving them a distribution of T_C as a whole. Oxidation was ruled out as the XRD patterns (particle size of $\sim$25μm) have not shown any peaks related to oxides.

B. Modelling Results

The Bean-Rodbell model considers the exchange constant to vary linearly with the unit cell volume, as described in the introduction. The total angular momentum, J, was calculated from saturation magnetization, M_s, measurements at 10 K up to 10 T, where $M_s = \rho_s g \mu_B J$. We have let
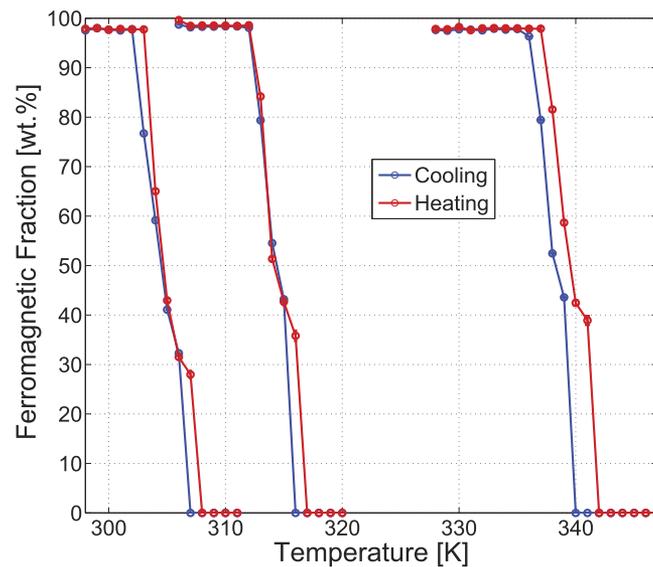

FIG. 3. FM fraction as a function of temperature determined from Rietveld refinement for the three different materials during the cooling and heating procedures.
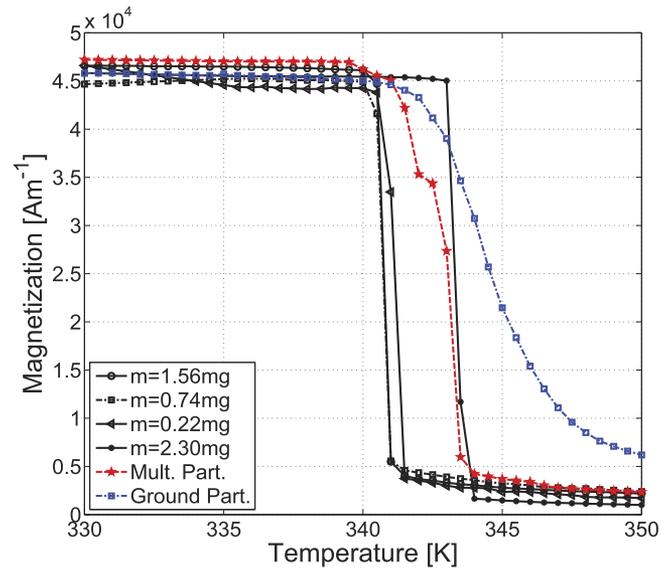
FIG. 4. Single particles and multiple particles isofield ($H_{app} = 0.01$ T) magnetization measurements, during the heating procedure.

three parameters vary: η, T_0 and $\sigma(T_0)$, where $\sigma(T_0)$ is the standard deviation of a normal distribution superimposed on T_0 to account for stoichiometric inhomogeneities.[15] Furthermore, from this normal distribution we can then calculate the FM fractions as the transition occurs. Moreover, the PM volume is constant neglecting the small thermal expansion in this temperature range. The fixed parameters were κ, J, ρ and ρ_s, with values of $3 \cdot 10^{-12}$ Pa^{-1}, 0.92, 7000 kgm^{-3} and $8.44 \cdot 10^{24}$ kg^{-1}, respectively.[9]

Figure 5 shows the unit cell volume as a function of the temperature for both the modelled and experimental results of the sample with $x = 0.25$. One may see the good agreement between the modelled and the measured data. The other compositions present as good agreement as the one shown here, and the obtained parameters are shown in Table I. One may see that the parameters are quite similar, and all materials have $\eta > 1$ i.e. they undergo a FOPT. The standard deviations are very similar as well, which is expected for a standardized materials processing technique.[16]
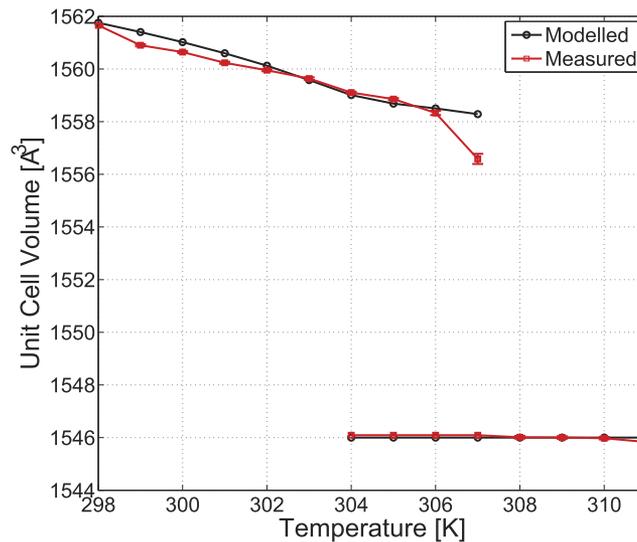

FIG. 5. Experimental and model results of volume as a function of temperature for the heating procedure of the material with $x = 0.25$.
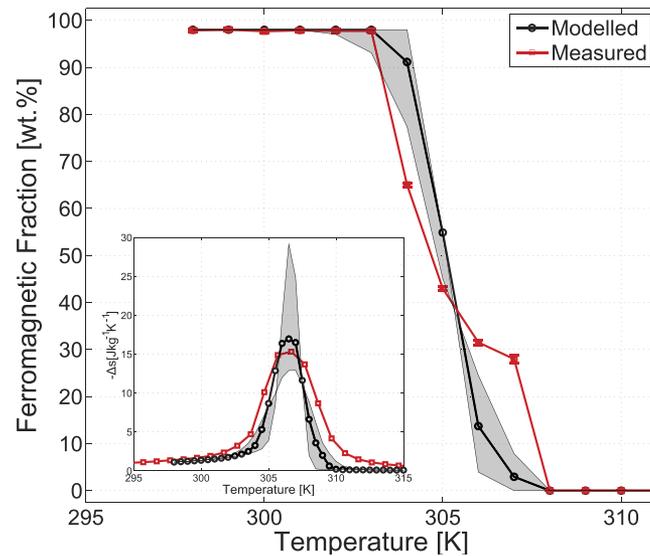
FIG. 6. Experimental and model results of FM fraction as a function of temperature for the heating procedure of the material with $x = 0.25$. The inset shows the Δs for $\mu_0 \Delta H = 1.0$ T. The shaded area in both graphs represents the region for $\sigma(T_0) \pm 0.5$ K.

Figure 6 shows the FM fraction for the composition with $x = 0.25$ during the heating procedure, comparing measurements with the modelled data. The shaded area represents a region with $\sigma(T_0) \pm 0.5$ K. The modelled results are as expected for a normally distributed function, however the measured data shows a more complex transition. Waske et al.[8] have shown that the volume change combined with microstructural features (grain boundaries arrangement) may play an important role in the transition itself. As the material transits from FM to PM, the stoichiometry distribution may lead to different T_C and therefore different parts of the sample have the transition at different temperatures. Morever the inset shows the Δs as function of the temperature for a field change of $\mu_0 \Delta H = 1.0$ T. The demagnetization factor was not considered in this case. The figure shows a good agreement between measurement and modelled data. More importantly, the results clearly shows that the distribution of T_0 has a major influence in the peak value of Δs.

IV. CONCLUSIONS

The phase transition of $La(Fe,Mn,Si)_{13}H_y$ for different compositions was evaluated by means of XRD. The results showed an increase of the unit volume volume change with decrease of x in $LaFe_{13-x-y}Mn_xSi_yH_{1.65}$. During the transition it was observed the presence of both FM and PM phases in a range of 6 K around each T_C. Magnetization measurements in single particles showed different T_C, another indication of stoichiometric distribution. Fitting the experimental data with Bean-Rodbell model indicates that all the three compositions studied presented FOPT as $\eta > 1$ for all of them.

ACKNOWLEDGMENTS

[1] A. Smith, Eur. Phys. J. H **38**, 507 (2013).

[2] A. Smith, C. R. H. Bahl, R. Bjørk, K. Engelbrecht, K. K. Nielsen, and N. Pryds, Adv. Energy Mater. **2**, 1288 (2012).

[3] J. D. Moore, K. Morrison, K. G. Sandeman, M. Katter, and L. F. Cohen, Appl. Phys. Lett. **95**, 252504 (2009).

[4] V. Basso, M. Kuepferling, C. Curcio, C. Bennati, A. Barzca, M. Katter, M. Bratko, E. Lovell, J. Turcaud, and L. F. Cohen, J. Appl. Phys. **118**, 053907 (2015).

[5] K. K. Nielsen and K. Engelbrecht, J. Phys. D: Appl. Phys. **45**, 145001 (2012).

[6] A. Fujita, S. Fujieda, K. Fukamichi, H. Mitamura, and T. Goto, Phys. Rev. B **65**, 014410 (2001).

[7] J. Lyubina, R. Schäfer, N. Martin, L. Schultz, and O. Gutfleisch, Advanced Mat. **22**, 3735 (2010).

[8] A. Waske, L. Giebeler, B. Weise, A. Funk, M. Hinterstein, M. Herklotz, K. Skokov, S. Fähler, O. Gutfleisch, and J. Eckert, Phys. Status Solidi RRL **9**, 136 (2015).

[9] L. Jia, J. R. Sun, H. W. Zhang, F. X. Hu, C. Dong, and B. G. Shen, J. Phys.: Condens. Matter **18**, 9999 (2006).

[10] C. P. Bean and D. S. Rodbell, Phys. Rev. **126**, 104 (1962).

[11] D. T. Cam Thanh, E. Brück, O. Tegus, J. C. P. Klaasse, T. J. Gortenmulder, and K. H. J. Buschow, J. Appl. Phys. **99**, 08Q107 (2006).

[12] K. K. Nielsen, H. N. Bez, L. von Moos, R. Bjørk, D. Eriksen, and C. R. H. Bahl, Rev. Sci. Instrum. **86**, 103903 (2015).

[13] H. M. Rietveld, J. Appl. Cryst. **2**, 65-71 (1969).

[14] J. Liu, J. Moore, K. Skokov, M. Krautz, K. Löwe, A. Barcza, M. Katter, and O. Gutfleisch, Scr. Mater. **67**, 584 (2012).

[15] N. G. Bebenin, R. I. Zainullina, and V. V. Ustinov, J. Appl. Phys. **113**, 073907 (2013).

[16] A. Barcza, M. Katter, V. Zellmann, S. Russek, S. Jacobs, and C. Zimm, IEEE Trans. Magn. **47**, 3391 (2011).